COUPLED HYDRO-MECHANICAL ANALYSIS OF FAULT REACTIVATION IN RESERVOIR

Sarita Maria de Figueiredo Souza Melo

sarita.figueiredo@hotmail.com

Lícia Mouta da Costa

licia@ufpe.br

Igor Fernandes Gomes

gomes@ufpe.br

Civil Eng. Dept., UFPE – Federal University of Pernambuco

Av. Acadêmico Hélio Ramos, s/n, 50740-530, Recife, Pernambuco, Brazil

Telmo Rosário Santos

telm_ro@hotmail.com

Instituto Superior Técnico

Av. Rovisco Pais 1, 1049-001, Lisboa, Portugal

Abstract. *Pressure increase inside a faulted reservoir, due to an advanced oil recovery method changes the stress state in its interior and the surrounding rocks, which can be irreversible, leading to the occurrence of new fractures and the reactivation of existing faults. Fault reactivation increases its permeability, which may create new paths for oil flow through overburden formations with high capillarity and low permeability, thereby compromising the performance of overburden reservoir rock. So fault reactivation can result in problems such as reducing oil production, oil exudation that migrates to the surface, leading to environmental problems and production facilities as well as surface subsidence problems, etc. Therefore, a previous studying of the allowed maximum pressure generated by the oil recovery is essential for fault reactivation analysis, as well as the model that best represents the fault material and its iteration with surrounding rocks. This paper presents a hydro-mechanical coupled analysis adopting as fault mechanical model Mohr-Coulomb with viscous regularization of plasticity through the Perzyna model.*

Keywords: *Fault reactivation, Hydro-mechanical coupling, Finite elements*

1 INTRODUCTION

Sealing faults are structures of great importance for the hydrocarbon trapping in the generation and migration processes (Soltanzadeh and Hawkes, 2008; Rutqvist et al, 2007). Due to its low permeability, fluid flow through the reservoir is not allowed from one side to another of the fault as well as fluid migration to other permeable zones of the geological formation.

The motion of faults within and on the surrounds of a petroleum reservoir can be induced in an exploitation process, by reducing the pore pressure and its effect over the normal effective stress and shear failure, and it is also a direct function of the stress state that acts on the field and on the fault surfaces. When the reactivation occurs, the fault permeability is increased, allowing the fluid to flow through it, compromising the hydraulic integrity of the cap rocks that seal the reservoir. Another aspect due to fault reactivation is the opening of fractures and the appearance of new flow zones through cap formations of high capillarity and low permeability (Gomes et al., 2012).

This problem can be safely studied based on a coupled hydro-geomechanical analysis tool with realist modeling of the constitutive behavior of the materials. Many researches involving hydro-mechanical numerical modeling of fault reactivation problems are being developed such in Rutqvist et al. (2007), Soltanzadeh and Hawkes (2008), Guimarães et al. (2009), Gomes et al. (2012), Rutqvist et al. (2013), among others.

In this paper a finite element procedure is presented that models fluid flow in an elastic deformable reservoir crossed by a geological fault in a coupled and full implicit way. Whether the fault is activated or not is governed by the hydro-mechanical boundary conditions of the problem and by the modeling of the elastovisccoplatic constitutive behavior of fault materials. The mechanical constitutive model used was Mohr-Coulomb (dilatancy considered) with viscous regularization of plasticity through the Perzyna's model (Heeres, 2001; Karaoulanis, 2003; Gomes et al., 2006).

2 MATHEMATICAL FORMULATION

The numerical analysis carried out in this paper used the “in house” finite element program CODE_BRIGHT (COupled DEformation, BRIne, Gas and Heat Transport) presented by Olivella et al. (1994), in which in the mechanical coupling, the hydraulic problem equations are solved together with the stress equilibrium equation, that features the geomechanical problem.

2.1 Hydraulic equation

Considering the porous medium saturated with a single fluid, the hydraulic problem is characterized by the mass balance equation of the fluid phase using Darcy´s Law and the addition of the mechanical term of coupling, as

$$\frac{\partial(\phi\rho_l)}{\partial t}+\nabla\left(\rho_l\mathbf{q}_l+\phi\rho_l\dot{\mathbf{u}}\right)=0 \tag{1}$$

where ρ_l is the liquid density and ϕ is rock porosity. In the flow term the component of porous medium deformation is described by the solid phase velocity, $\dot{\mathbf{u}}$ and the fluid flow relative to solid phase is described by Darcy law, considering one single fluid, given by

$$\mathbf{q}_l = -\frac{\mathbf{k}}{\mu_l}\left(\nabla p_l - \rho_l \tilde{\mathbf{g}}\right). \tag{2}$$

where $\tilde{\mathbf{g}}$ is the gravity vector, ∇p_l is pressure gradient and μ_l is liquid viscosity. The intrinsic permeability tensor is represented by $\mathbf{k}$ (considered isotropic in the present paper).

Porosity ϕ and intrinsic permeability $\mathbf{k}$, are porous medium properties, which can be defined as coupling variables, once they are updated by the geomechanical model and introduce the effect of deformation in flow equation.

2.2 Mechanical constitutive model

In the adopted formulation, the mechanical problem is defined by the stress equilibrium equation (Eq. (3)), together with Terzaghi effective stress principle (Eq. (4)). The mechanical behavior is controlled by the effective stresses **σ'** (Eq. (5)), which increases as pore pressure decreases.

$$\nabla\boldsymbol{\sigma} + \mathbf{b} = 0 \tag{3}$$

$$\boldsymbol{\sigma} = \boldsymbol{\sigma}' + \mathbf{m}p_l \tag{4}$$

$$\nabla\boldsymbol{\sigma}' + \mathbf{m}\nabla p_l + \mathbf{b} = 0 \tag{5}$$

where $\boldsymbol{\sigma}$ is the symmetric tensor of total stresses, **b** is the body force vector and **m** is na auxiliary vector ($\mathbf{m}^T$= 1,1,1,0,0,0).

The mechanical constitutive model adopted is Mohr-Coulomb with viscous regularization of plasticity through the Perzyna's model. The increment of effective stresses and strains are related by

$$\dot{\boldsymbol{\sigma}}' = \mathbf{D}_{\mathbf{ep}}\dot{\boldsymbol{\varepsilon}} \tag{6}$$

where $\mathbf{D}_{\mathbf{ep}}$ is an elastoplastic constitutive tensor, obtained as a function of elastic tensor and gradients of flow law $F(\boldsymbol{\sigma},\kappa)$ and plastic potential $P(\boldsymbol{\sigma},m)$ in respect to stress estate, where for associated plasticity (adopted in this work) $F(\boldsymbol{\sigma},\kappa) = P(\boldsymbol{\sigma},m)$.

Total strain is composed by the sum of an elastic and a viscoplastic strain.

The flow rule adopted in Perzyna's model (Heeres, 2001; Karaoulanis, 2003; Gomes et al., 2006) is given by Eq. (7), that consists in the addition to the plastic analysis of a viscoplastic multiplier λ, which considers a viscous parameter η and a overstress function $\langle\phi(F(\boldsymbol{\sigma},\kappa))\rangle$ that is a penalty function of plasticity and depends of the rate independent yield surface (Eq. (8)).

$$\dot{\varepsilon}^{vp} = \lambda\frac{\partial F(\boldsymbol{\sigma},\kappa)}{\partial\boldsymbol{\sigma}} = \frac{\langle\phi(F(\boldsymbol{\sigma},\kappa))\rangle}{\eta}\frac{\partial F(\boldsymbol{\sigma},\kappa)}{\partial\boldsymbol{\sigma}} \tag{7}$$

$$\langle \phi(F) \rangle = \begin{cases} \phi(F) & \text{if } \phi(F) \geq 0 \\ \phi(F) & \text{if } \phi(F) < 0 \end{cases} \tag{8}$$

As discussed by Heeres *et al* (2002), the widely-used expression for ϕ is described in Eq. 9, where α is commonly chosen as the initial yield stress, and N is a calibration parameter that should satisfy $N \geq 1$.

$$\phi(F) = \left(\frac{F}{\alpha} \right)^N \tag{9}$$

The yield function is expressed by:

$$F(\boldsymbol{\sigma}', k) = J - \left(\frac{c'}{\tan(\phi')} + p' \right) G(\theta) = 0 \tag{10}$$

with

$$g(\theta) = \frac{sen(\phi')}{\cos(\theta) + \frac{sen(\theta) sen(\phi')}{\sqrt{3}}} \tag{11}$$

where p', J and θ are the stress invariants defined as effective mean stress, deviatory stress and Lode's angle. c' and ϕ' are effective cohesion and friction angle respectively.

2.3 Hydro-mechanical coupling

An important characteristic of the used formulation is the coupling between porosity variation and intrinsic permeability changes. Porosity variation is computed by using the solid balance equation, given by

$$\frac{D\phi}{Dt} = \frac{(1-\phi)}{\rho_s} \frac{D\rho_s}{Dt} + (1-\phi) \frac{d\varepsilon_v}{dt} \tag{12}$$

where ε_v is the volumetric strain and ρ_s the density of the solid phase.

The determination of the permeability as a function of rock deformation is a complex function that depends on the elastic and inelastic regime in which the material is subjected. For the elastoplastic Mohr-Coulomb model a linear law limiting the maximum value of permeability was adopted as a function of shear plastic strain (Fig. 1), that is directly related to the volumetric plastic strain for a given the dilation angle.

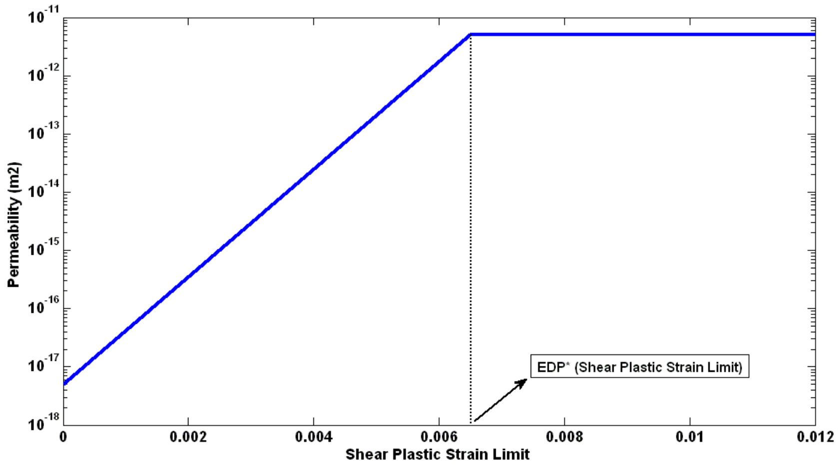

Figure 1. Permeability law associated to Mohr-Coulomb model.

3 APPLICATION

This paper presents the hydro-mechanical analysis of a synthetic problem of an oil reservoir crossed by a sealing fault. The analysis considers 2D plane strain condition, with the geometry illustrated in Fig. 2, which consists of overburden, reservoir, underburden and the sealing fault, which is considered as a homogeneous continuous medium.

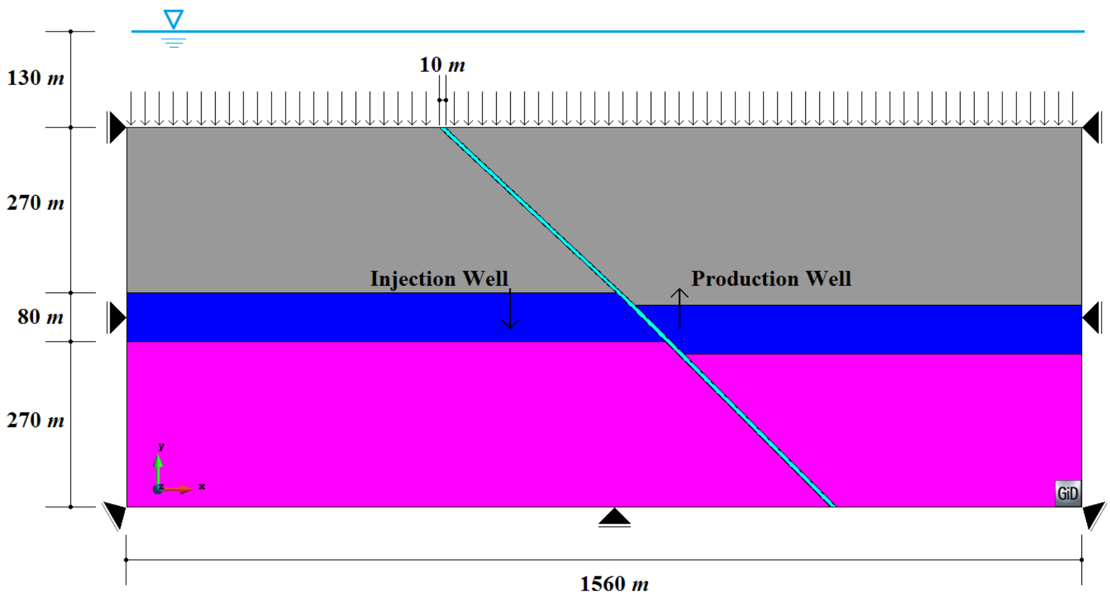

Figure 2. Geometry and boundary conditions.

Boundary conditions are also indicated in Fig. 2. Considering the reference level the sea water level (zero depth), boundary conditions applied on the sea bed are such that lead to a state of effective stress zero in this region. It was assumed an injector well located 232 m at the left of the fault and at a depth of 469m, operating with a bottom hole pressure of 3.8 MPa above original pressure, and a production well, 46 m at the right of the fault and at a depth of 449 m, operating with a pressure of -2.0 MPa.

The finite element mesh adopted in the analysis is composed by 4191nodes and 8266 linear triangular elements (Fig. 3). Fluid compressibility and density are, respectively, 3.4e^{-6} MPa^{-1} and 710.0 kg/m^3. The material properties adopted are presented in Table 1. Overburden, reservoir and underburden rocks behave as elastic materials, while sealing fault is modeled by Mohr-Coulomb with viscous regularization of plasticity.

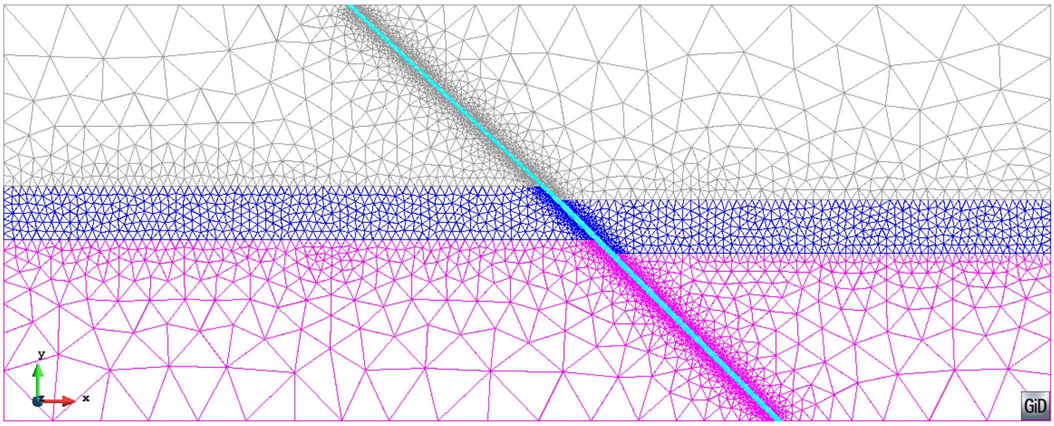

Figure 3. Finite element mesh adopted in the analysis.

Table 1. Material properties

Rock properties	Overburden	Underburden	Reservoir	Fault
Young Modulus (MPa)	1900	4200	9200	8400
Cohesion (MPa)	2.3	2.3	5.8	0.5
Friction angle	26º	26º	30º	23º
Permeability (m^2)	1.0e-30	1.0e-30	5.0e-12	5.0e-25
Porosity	0.20	0.18	0.30	0.25

In this work it was carried out a sensitivity analysis of Perzyna viscosity parameter adopted to the fault material. Four different values are considered for the viscosity parameter η, 10^3, 10^4, 10^5 and 10^6.

Shear plastic strain is the indicator of the reactivation process. It controls the evolution of fault permeability in geomechanical constitutive model. In Fig. 4 it is indicated an element in the fault where numerical results will be evaluated for the reactivation process. Figure 5 presents the evolution of plastic strains for the cases carried out. With the viscosity parameter increase it takes to smooth in stress strain response and inelastic strain evolution, where the stress is allowed to go outside the yield surface, which effect is known as overstress. The case corresponding to the lowest η presents the lowest viscous regularization of plasticity, leading to a similar rate independent response.

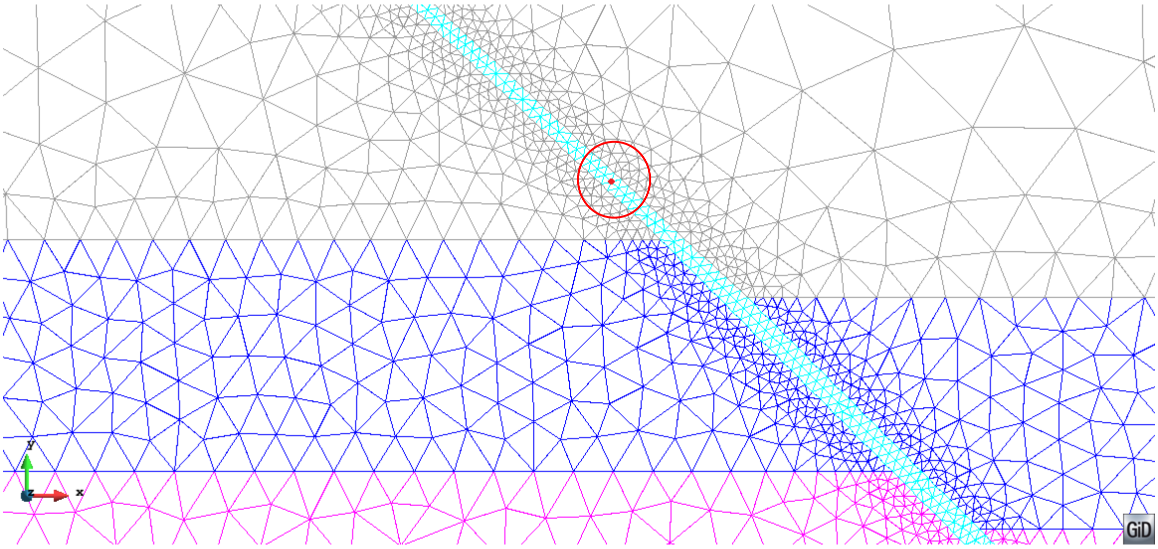

Figure 4. Element considered for evaluation of fault reactivation

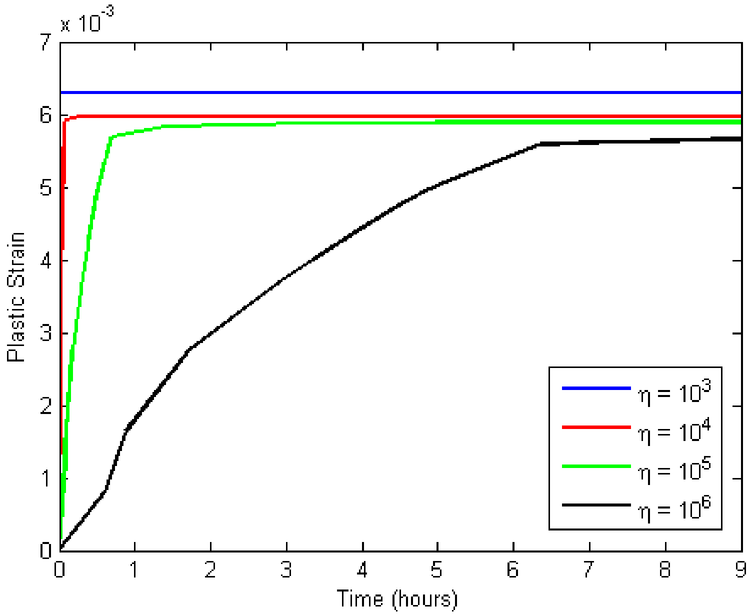

Figure 5. Evolution of plastic strain with time.

Figure 6 presents the permeability evolution for the examples analyzed. It can be seen a marked increasing in permeability, according to the plastic strain achieved (Fig. 5) and following the function presented in Fig. 1.

Liquid pressure increases until fault achieve maximum shear plastic strain, following by a sudden pressure decreasing and stress redistribution to the neighborhood, stabilizing pressure at different levels for each example, as indicated in Fig. 7.

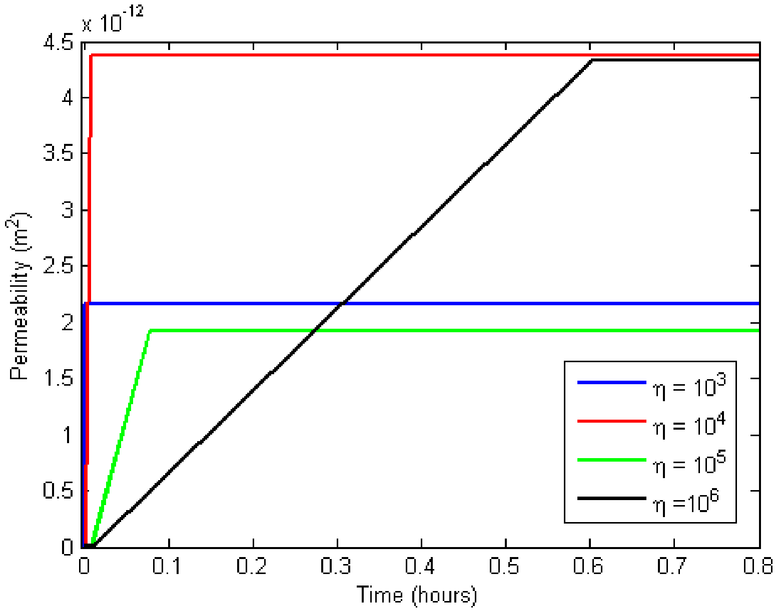

Figure 6. Evolution of intrinsic permeability with time.

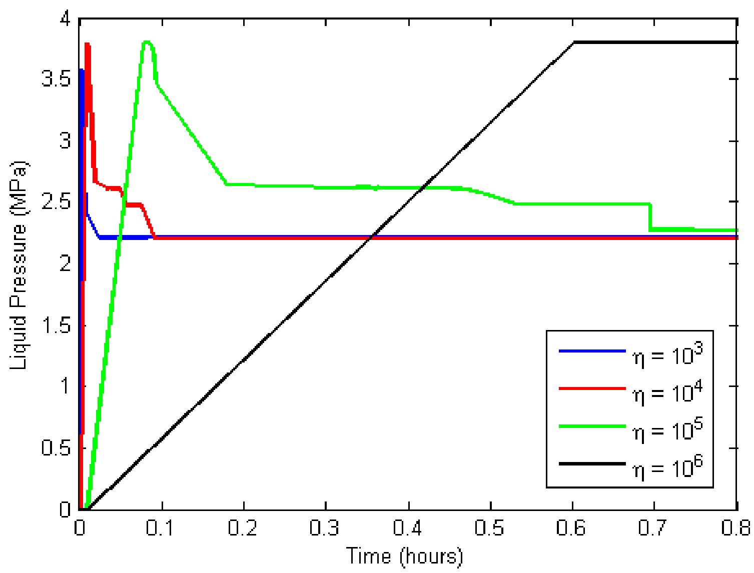

Figure 7. Evolution of liquid pressure with time.

When an element develops shear plastic strain and its permeability increases, fluid flow takes place allowing the pressurization of the nearby elements and the propagation of pressure along the fault. This process can lead to fluid flow through the fault, and towards the right side of reservoir. Figures 8 to 12 present the results for the examples for $\eta = 10^3$ and $\eta = 10^6$ considering a time analysis of ten hours.

For $\eta = 10^3$ it was observed that stabilization occurs for a time of three hours. Distribution of plastic strain, permeability and liquid pressure (Fig. 8, 9 and 10) do not change from three until ten hours (final time analysis).

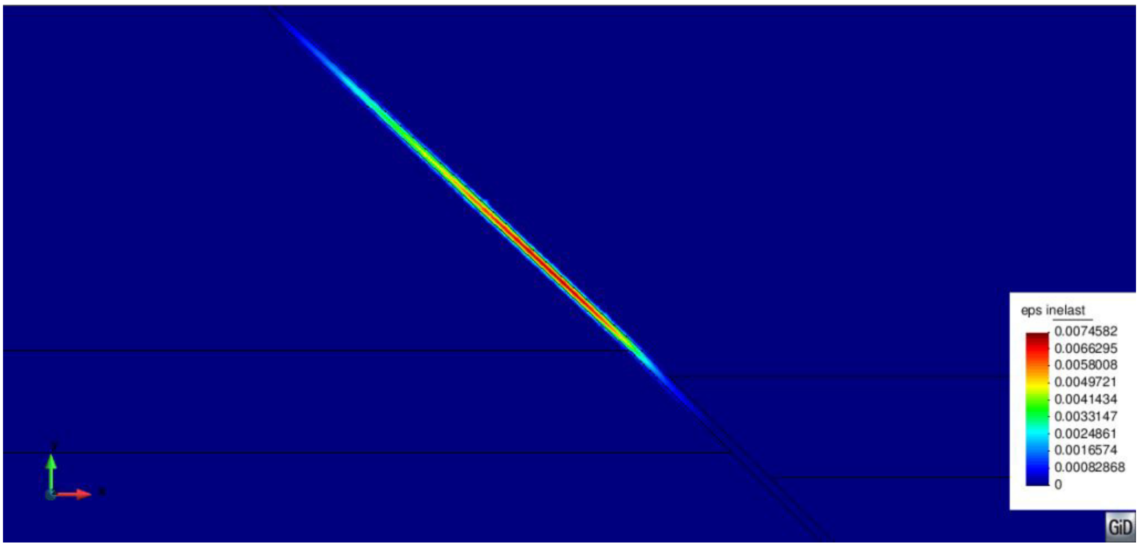

Figure 8. Final plastic strain distribution for $\eta = 10^3$.

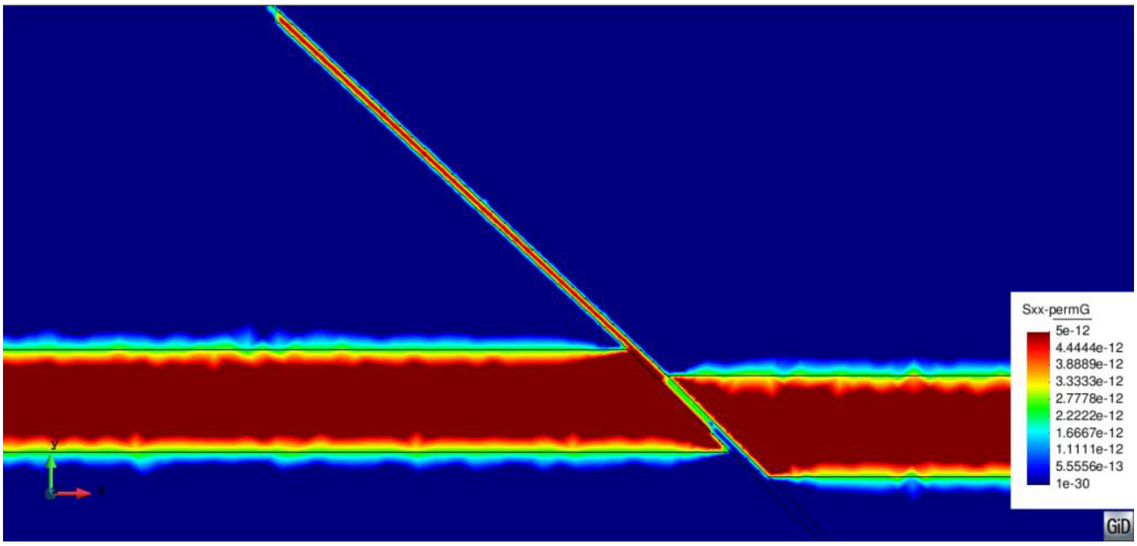

Figure 9. Final permeability distribution for $\eta = 10^3$.

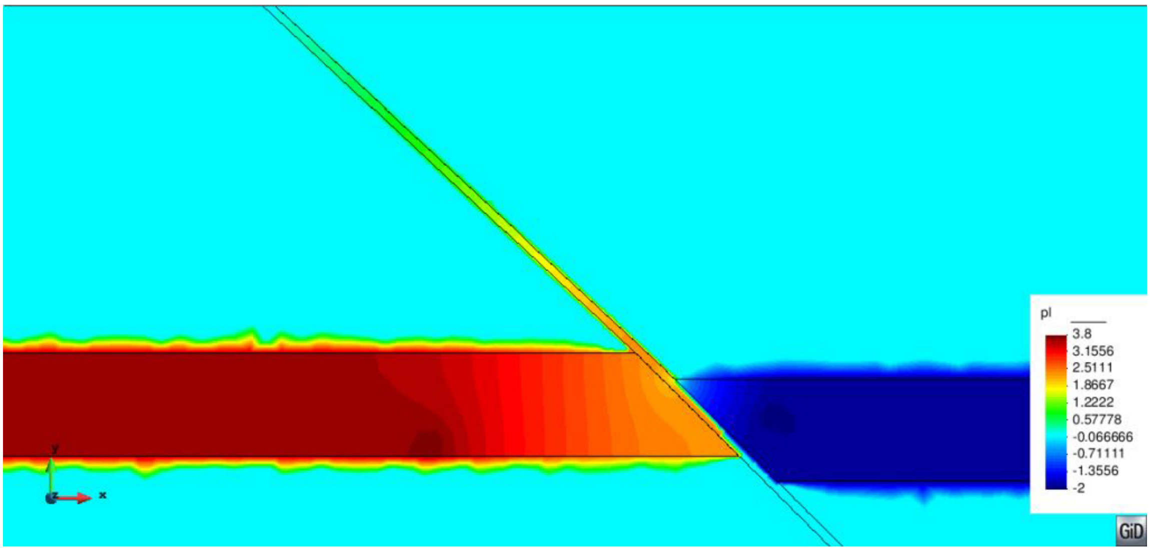

Figure 10. Final liquid pressure distribution for $\eta = 10^3$.

For $\eta = 10^6$ the inelastic strain evolution is smoothed and slower in relation to lowest values of η (Fig. 11). The stresses that are developed in the fault material are allowed to be larger than the yield stress as function to η increase. Is possible reaches to more accurately stress redistribution result after the element reactivation. As final result, the fault is crossed by the fluid to the right side of the reservoir and also towards sea bed.

Pore pressure variation induces significant changes in the stress state leading to yielding and the development of plastic strains. Figure 13 shows the distribution of shear stress for the example with for $\eta = 10^3$. It can be seen the concentration of shear stress in the fault zone. Vertical displacement distribution is presented in Fig. 14.

Figure 15 shows the deformed mesh and vertical displacement distribution for the example with for $\eta = 10^6$.

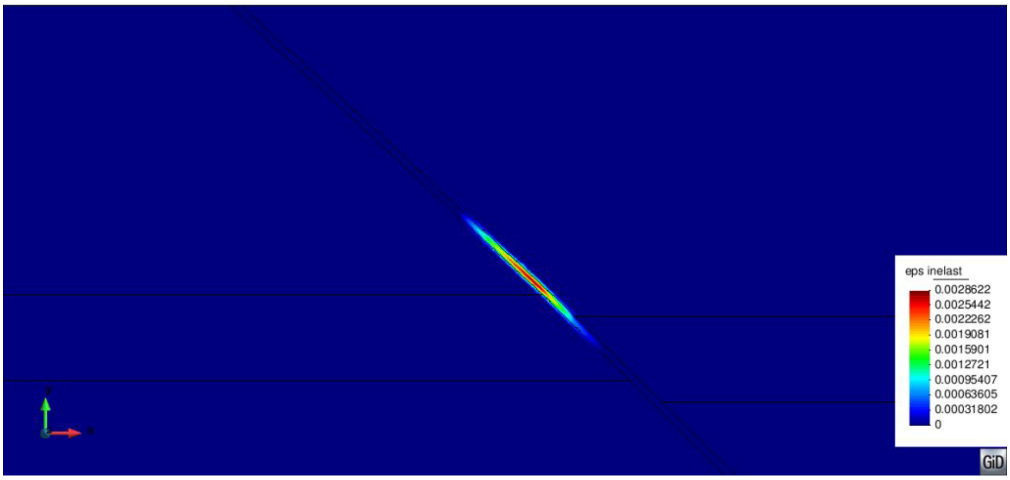

(a)

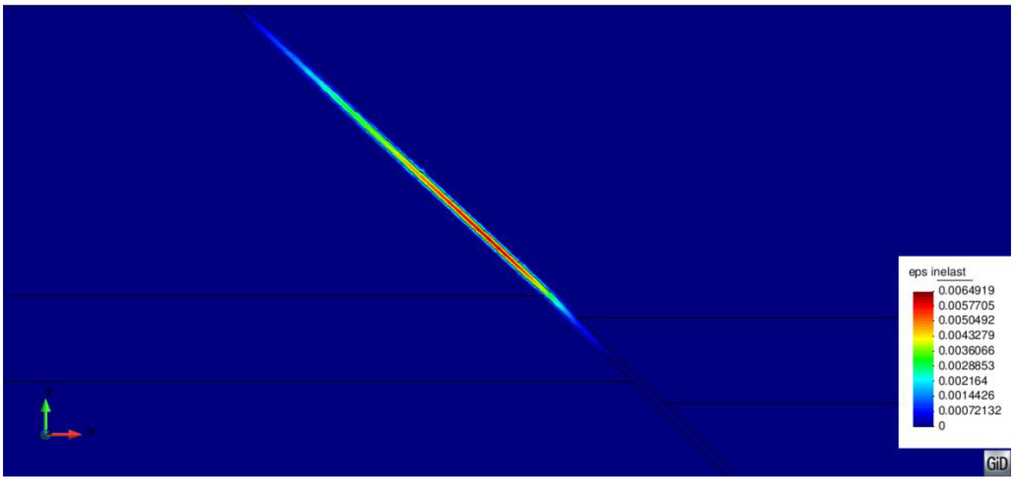

(b)

Figure 11. Plastic strain distribution for $\eta = 10^6$: a) at three hours; b) Final time;

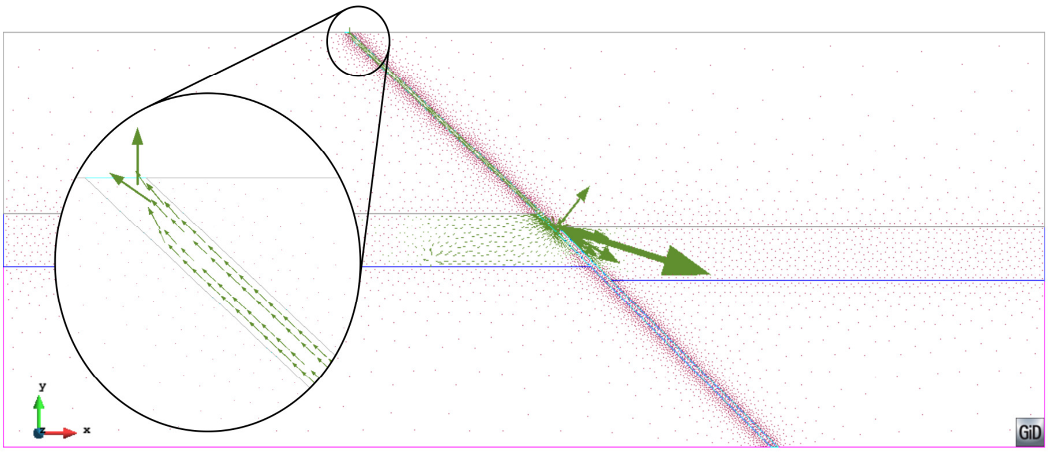

Figure 12.Fluid flow vectors for $\eta = 10^6$.

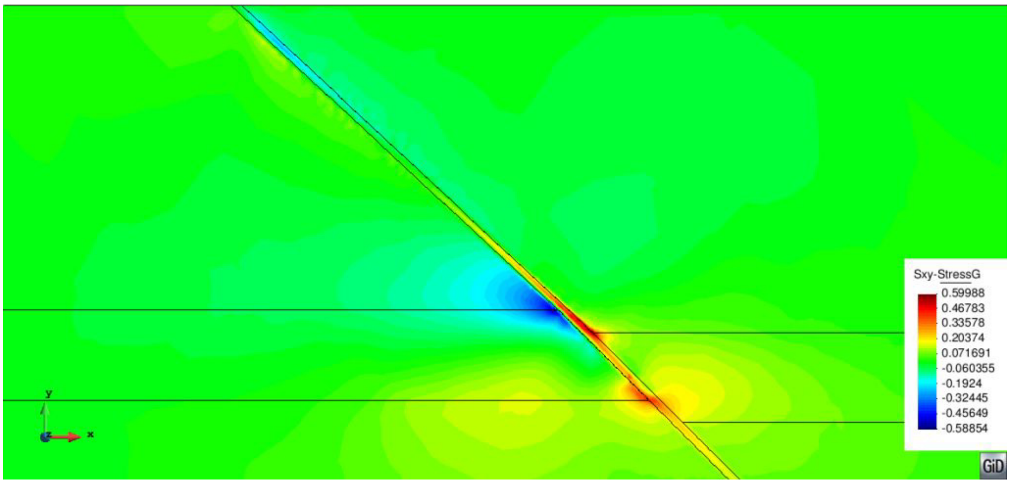

Figure 13. Final shear stress distribution for η = 10³.

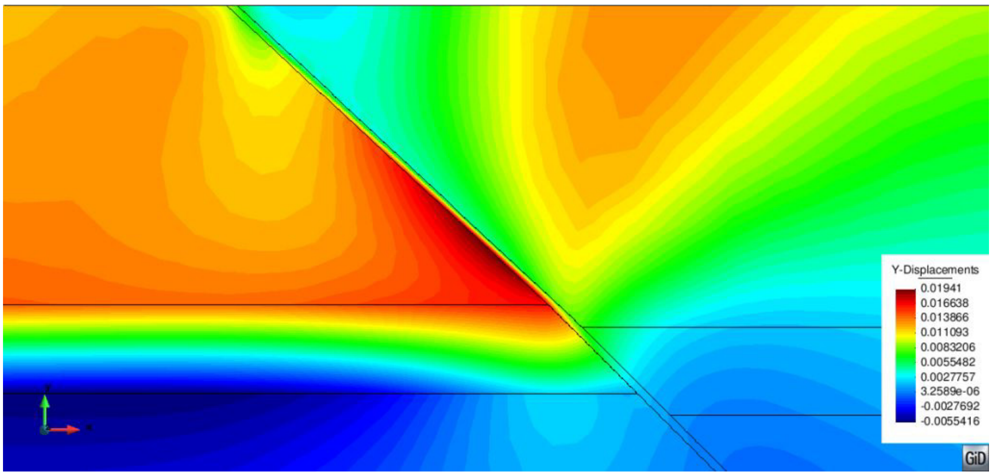

Figure 14. Final vertical displacement distribution for η = 10³.

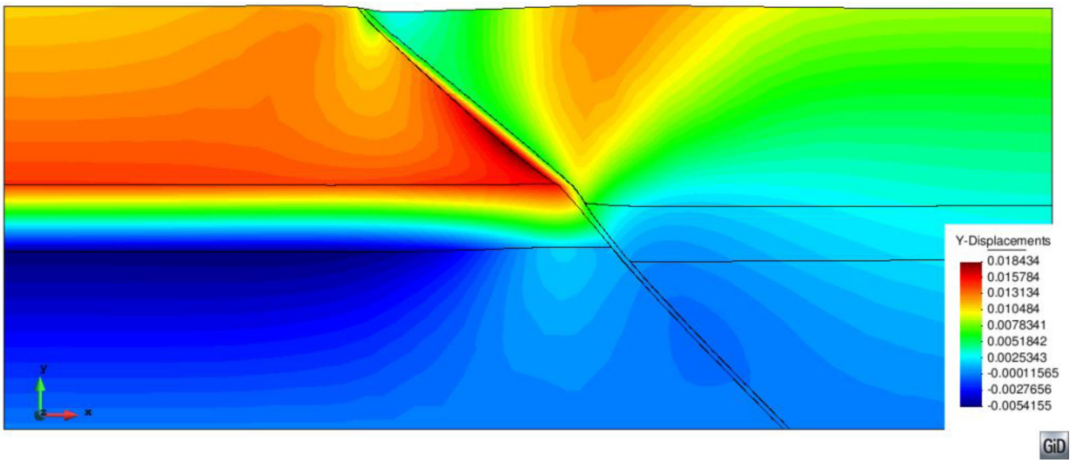

Figure 15. Final vertical displacement distribution and deformed geometry for η = 10⁶.

CONCLUSION

In this work it was analyzed a rate-dependent behavior of fault reactivation in a coupled hydro mechanical simulation. It can be described within the framework of elasto-viscoplasticity where the total strain rate is decomposed into two parts: a reversible and an irreversible and rate-dependent deformation. For the Perzyna's model a plasticity regularization is provided and the stresses are allowed to go to out of the yield surface, an effect called as overstress.

For different values of regularization viscoplastic parameter η, the overstress effects is influenced and leads to a stresses development allowed to be larger than the yield stress. It is assumed that the most adequately value of viscoplastic parameter η adopted in this sensibility analysis is 10^3 because a rate-independent elastoplastic model is recovered if $\eta \rightarrow 0$. Therefore, the viscoplastic penalty is reduced and values of η closer to zero can lead to numerical convergence troubles in problems like fault reactivation which are characterized by material rupture. In the case of fault reactivation, it's important to understand the fluid pressure distribution after the material failure as function of time due to stress redistribution. Other great importance of a viscoplastic material modeling, is that the numerical algorithm becomes more stable and lead to less convergence problems because stresses above the yield limit are allowed and not ruled out as in classical plasticity (Karaoulanis, 2003).

ACKNOWLEDGEMENTS

The authors would like to acknowledge the financial support for this research given by CNPq (National Research Council, Brazil), Petrobras and PRH-26(ANP).

REFERENCES

Costa, C. G. & Borges, L. M. S. A., 2005. A mixed model and an algorithm for viscoplasticity. *18th International Congress of Mechanical Engineering.* Ouro Preto, Brasil.

Gomes, I. F., Guimarães, L. J. N., Pontes, I. D. S., Costa, L. M., 2012. Modeling fluid flow in stress sensitive petroleum reservoir considering fault reactivation problem. *10th World Congress on Computational Mechanics.* São Paulo, Brasil.

Gomes, I. F., Guimarães, L. J. N. & Pontes Filho, I. D. S., 2006. Implementação de modelo viscoplástico de Perzyna pelo método explícito de Runge-Kutta-Dormand-Price**.** *XXVII Iberian Latin Congresso on Computational Methods in Engineering*. Belém, Brasil.

Guimarães, L. J. N., Gomes, I. F., Fernandes, J. P. V., 2009. Influence Of Mechanical Constitutive Model On The Coupled Hydro-Geomechanical Analysis Of Fault Reactivation. *2009 SPE Reservoir Simulation Symposium. SPE 119168.* The Woodlands, Texas, U.S.A.

Heeres, O. M., 2001. Modern Strategies for the Numerical Modeling of the Cyclic and Transient Behavior of Soils. *Doctor Thesis, Civiel Ingenieur, Technische Universiteit Delft*, Netherlands.

Heeres, O., Suiker, A., Borst, R., 2002. A Comparison between the Perzyna Viscoplastic Model and the Consistency Viscoplastic Model. *European Journal of Mechanics A/Solids*, 21, pp. 1-12.

Karaoulanis, F., 2003. Viscoplastic Material Modelling. *Master Thesis, Computacional Mechanics, Lehrstuhl für Bauinformatik, Technische Universität München*, München.

Olivella, S., J. Carrera, A. Gens & E. E. Alonso. 1994. Nonisothermal Multiphase Flow Of Brine And Gas Through Saline Media. *Transport in Porous Media*, 15, 271-293.

Rutqvist, J., Birkholzer J., Cappa F. & Tsang C. F., 2007. Estimating maximum sustainable injection pressure during geological sequestration of CO_2 using coupled fluid flow and geomechanical fault-slip analysis. *Energy Conversion and Management*, 48, (March). pp. 1798-1807.

Rutqvist, J., Rinaldi, A. P., Cappa F. & Moridis, G. J., 2013. Modeling of fault reactivation and induced seismicity during hydraulic fracturing of shale-gas reservoirs. *Journal of Petroleum Science and Technology*, 107, pp. 31-34.

Soltanzadeh, H., Hawkes, C. D., 2008. Semi-analytical models for stress change and fault reactivation induced by reservoir production and injection. *Journal of Petroleum Science and Engineering*, 60, pp. 71-85.